ACS APPLIED MATERIALS & INTERFACES

Research Article

www.acsami.org

MoS_2 Nanolayers Grown on Carbon Nanotubes: An Advanced Reinforcement for Epoxy Composites

Keqing Zhou,[†] Jiajia Liu,[†] Yongqian Shi,[†] Saihua Jiang,[‡] Dong Wang,[†] Yuan Hu,*[,†] and Zhou Gui*[,†]

[†]State Key Laboratory of Fire Science, University of Science and Technology of China, Hefei, Anhui 230026, People's Republic of China

[‡]School of Mechanical and Automotive Engineering, South China University of Technology, Guangzhou 510641, People's Republic of China

Supporting Information

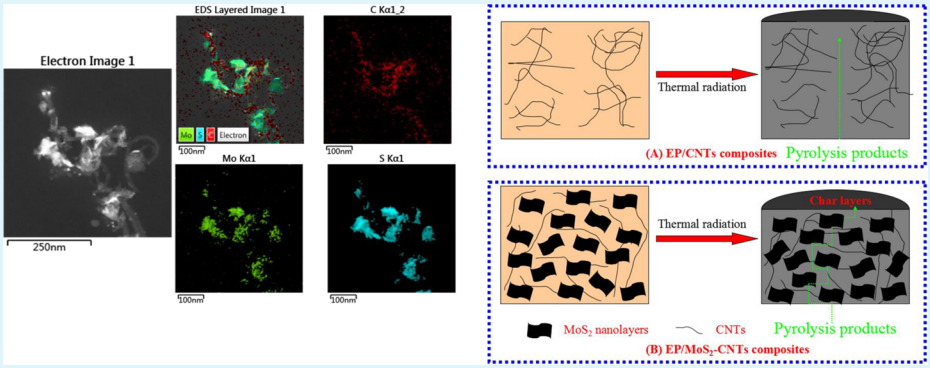

ABSTRACT: In the present study, carbon nanotubes (CNTs) wrapped with MoS_2 nanolayers (MoS_2−CNTs) were facilely synthesized to obtain advanced hybrids. The structure of the MoS_2−CNT hybrids was characterized by X-ray diffraction, Raman spectroscopy, scanning electron microscopy, and transmission electron microscopy measurements. Subsequently, the MoS_2−CNT hybrids were incorporated into EP for reducing fire hazards. Compared with pristine CNTs, MoS_2−CNT hybrids showed good dispersion in EP matrix and no obvious aggregation of CNTs was observed. The obtained nanocomposites exhibited significant improvements in thermal properties, flame retardancy and mechanical properties, compared with those of neat EP and composites with a single CNT or MoS_2. With the incorporation of 2.0 wt % of MoS_2−CNT hybrids, the char residues and glass transition temperature (T_g) of the EP composite was significantly increased. Also, the addition of MoS_2−CNT hybrids awarded excellent fire resistance to the EP matrix, which was evidenced by the significantly reduced peak heat release rate and total heat release. Moreover, the amount of organic volatiles from EP decomposition was obviously decreased, and the formation of toxic CO was effectively suppressed, implying the toxicity of the volatiles was reduced and smoke production was obviously suppressed. The dramatically reduced fire hazards were generally ascribed to the synergistic effect of MoS_2 and CNTs, containing good dispersion of MoS_2−CNT hybrids, catalytic char function of MoS_2 nanolayers, and physical barrier effects of MoS_2 nanolayers and CNT network structure.

KEYWORDS: *MoS_2, nanolayers, CNTs, epoxy resin, thermal properties, fire hazards*

1. INTRODUCTION

EP is one of the most important thermoset polymers, which are widely used in the fields of adhesive, coating, potting, electronic/electrical insulation, and composite applications, because of its outstanding mechanical stiffness and toughness, good solvent and chemical resistance, excellent thermal and mechanical stabilities, and superior adhesion.[1−3] However, the numerous advantages of EP resins could not cover up one of the major drawbacks: its inherent flammability and high yield of toxic smoke during combustion, which restricts its application in many fields for safety consideration. Thus, it is valuable to promote the thermal stability and reduce the fire hazards of EP composites. Many approaches have been exploited to improve the fire resistance of EP. In previous work, EP had been endowed with excellent fire resistance by incorporating halogen-containing flame retardants. However, the addition of halogenated flame retardants will produce toxic and corrosive gases during combustion, which is adverse to the environments and human health.[4] Therefore, it is of great significance to develop halogen-free flame retardants that can reduce the fire hazards of the EP composites effectively.

Recently, nanoparticles such as nanoclay, carbon nanotube, carbon nanofiber, graphene and polyhedral oligomeric silsesquioxanes have drawn intensive interest and are

Received: October 22, 2014
Accepted: March 5, 2015
Published: March 5, 2015

DOI: 10.1021/acsami.5b00762
ACS Appl. Mater. Interfaces 2015, 7, 6070−6081

considered to be potential fillers for improving flame retardancy and other physical properties simultaneously at low loading.[5,6] Because of the superior structural, conductivity, mechanical, and thermal properties, carbon nanotubes (CNTs) show great potential in various applications ranging from nanodevices to nanocomposites.[7] CNTs have been proved to be advanced multifunctional fillers in polymer-based nanocomposites. In recent works, the role of CNTs in the improvement of thermal stability and flame resistance of polymer matrices had become one of the hot topics. The improved flame resistance was ascribed to the formation of a continuous, free-standing nanotube network-structured protective layer which can act as a thermal shield to prevent energy feedback from the flame.[8] In general, the CNTs have shown more promising thermal and fire resistance properties in thermoplastics such as EVA, PS, PMMA, PA-6, LDPE, and PP.[8−13] In the case of brittle thermosetting polymers, such as epoxy, the improvement in flame retardancy properties using CNTs has been shown to be limited. To the best of our knowledge, previous works on EP/CNTs composites mainly concentrated on mechanical and electrical performances of the composites,[14−16] and rarely involved the research of thermal and flame retardant performance.[4,17]

Generally speaking, the flame retardancy efficiency of the CNTs is closely linked to its dispersibility in the polymeric matrix, which is the key factor to regulating the network structure and the consequent barrier effect against flame.[8] However, to obtain a complete network, good dispersion and strong interfacial interaction between the CNTs and polymer matrices have to be considered, but actually, the uniform dispersion of CNTs in polymer matrix is not easy to obtain because of the insolubility of CNTs and the inherently poor compatibility between CNTs and polymer matrices, the agglomeration and entanglement of CNTs owing to strong van der Waals forces and $\pi-\pi$ interactions, which limited the enhance effect of CNTs in polymer nanocomposites.[18,19] These obstacles can be ruled out by oxidation or covalent functionalization, or introduction of active chemical additives and other nanoparticles on the surface of CNTs.[20] For instance, HDPE coated MWCNTs exhibit homogeneous dispersion in EVA and result in a decrease of the PHRR.[9] Fang et al. has successfully prepared intumescent flame retardant grafted CNTs, which show good dispersion and fire resistance in ABS resin.[7] In addition, a new strategy has been proposed in recent work, which involves the addition of another kind of nanofiller play a role in synergy with CNTs, the incorporation of additional nanofiller can not only promote the formation of CNTs conductive network but also provide the other novel performances to polymer matrices. For example, it has indicated that introduction of MMT may improve the dispersity of MWCNTs in different media and the presence of clay promotes dispersity of MWCNTs, which is conducive to enhance electrophysical, mechanical, rheological, and thermal properties of different composites.[21−25] Fang et al. has shown that the combination of C_{60} and CNTs not only led to good dispersion of CNTs, but also resulted in excellent synergistic effects in the thermal, mechanical properties, and fire resistance of polypropylene.[26]

Another famous nanostructural material, which has been widely used in various applications, is layered MoS_2. Compared with 1D CNTs, layered MoS_2 is one kind of 2D nanomaterials which has been intensively studied as nanofillers for prepration of polymer nanocomposites in the past few years.[27−34] In our previous work, the incorporation of MoS_2 can improve the thermal stability and flame retardancy of the polymer matrices such as PVA, PS, and PMMA,[28−34] but the efficiency still needs to be optimized. For both 1D and 2D nanofillers, homogeneous dispersion and strong interfacial interactions with the polymer matrix are the most important issue which can maintain the intrinsic properties of nanofillers.[19,35] A large amount of research works have been focused on functionalization and dispersion of CNTs[36,37] and MoS_2[32,38,39] in different polymer matrix. In recent work, polymer nanocomposites based on nanohybrids that comprise two or more kinds of nanofillers have attracted intensive attention, because of their effective enhancement effects on mechanical, electrical, and thermal conductivity properties of the composites.[40,41] The realization of previous hybrids of C_{60} and graphene[42] provided us a novel route to decorate layered MoS_2 on the surface of CNTs, the deposited MoS_2 nanolayers can suppress the agglomeration of CNTs in the nanohybrids. Furthermore, synergistic effects between CNTs and MoS_2 can be anticipated to have potential applications in improvement of the dispersibility, thermal, mechanical properties and reducing fire hazards of EP composites. To the best of our knowledge, the previous works are mainly focused on investigate the electrochemical performances of the MoS_2−CNT hybrids,[43−46] and no reports about the combination of MoS_2 and CNTs for reducing the flammability of polymers have been published since the discovery of CNTs and MoS_2.

In this paper, we designed a novel route to decorate MoS_2 on the surface of CNTs to form a new interface between epoxy and CNTs, the deposited MoS_2 nanolayers can suppress the agglomeration of CNTs, which can improve the dispersibility of CNTs in epoxy matrices. In addition, the incorporation of MoS_2−CNTs nanohybrids results in significant improvements in char formation, thermal properties, flame retardancy, and mechanical properties, compared with those of neat EP and composites with a single CNTs, MoS_2 or mixture of CNTs and MoS_2. Moreover, the amount of releasing organic volatiles from EP decomposition was dramatically decreased, and the formation of toxic CO was effectively suppressed, implying the toxicity of the volatiles was reduced and smoke production was obviously suppressed. In the end, a novel combined flame retardant mechanism had been proposed.

2. EXPERIMENTAL SECTION

The concentrated sulfuric acid, nitric acid, $Na_2MoO_4{\cdot}2H_2O$ (AR), L-cysteine (AR), curing agent (DDM, AR), and NaOH (AR) were obtained from the Sinopharm Chemical Reagent Co., Ltd. Bisphenol-A type EP was purchased from shixian Chemical Industry Co., Ltd. The MWCNTs (degree of purity >95%) were obtained from Beijing DK Nano technology Co., Ltd.

2.1. Preparation of MoS_2−CNTs Hybrids. The MWCNTs were first modified with concentrated sulfuric acid and nitric acid (3:1 by volume) at 60 °C for 4 h and then the MoS_2−CNT hybrids were prepared as follows:[43] first, 0.4 g of acid treatment CNTs was ultrasonic dispersed in 300 mL of distilled water for 1 h. Then 1.2 g of $Na_2MoO_4{\cdot}2H_2O$ was dissolved in 20 mL of deionized water and then incorporated into the suspension of CNTs. After adjusting the pH value to 6.0 with 0.1 M NaOH, 3.2 g of L-cysteine was dissolved in 30 mL of distilled water and then introduced. The resultant mixture was diluted with distilled water to 400 mL and violently stirred with a speed of 2000 rpm for about 1 h. The mixture was then transferred into a 500 mL Teflon-lined stainless steel autoclave and heated at 180 °C for 48 h. The autoclave was left to cool naturally to room temperature, and then the product MoS_2−CNT hybrids were collected by centrifugation at 5000 rpm for 8 min, washed several times with

DOI: 10.1021/acsami.5b00762
ACS Appl. Mater. Interfaces 2015, 7, 6070−6081

distilled water (300 mL) and absolute ethanol (100 mL), and dried at 80 °C in a vacuum overnight. The yield of the MoS_2−CNTs nanohybrids was about 90%. The MoS_2 nanolayers were synthesized by a similar procedure in the absence of CNTs.

2.2. Preparation of EP/MoS_2−CNTs Composites. A typical preparing procedure for EP composites containing 2 wt % MoS_2−CNT hybrids is described as follows: 1.2 g of MoS_2−CNT hybrids were added into 100 mL of acetone solution with ultrasonication to prepare a uniform suspension in an ice water bath. Then, 50.0 g of EP was melt at 95 °C and then poured into the above suspension under mechanical stirring with a high speed of 3000 rpm for 6 h. Then the mixture was placed in an oil bath at 100 °C for 24 h to remove the acetone under mechanical stirring. Ten grams of DDM was melted at 110 °C and then dumped into the related mixture under mechanical stirring for 5 min. Finally, the EP/MoS_2−CNTs composites were cured at 100 and 150 °C for 2 h, respectively. In the end, the composites were placed to cool to room temperature. Moreover, a similar procedure was used to prepare pure EP, EP/CNTs, EP/MoS_2 composites except changing the kinds of additives. The content of the nanofillers in all the samples was consistent with 2 wt %. In addition, the EP composites containing 1 wt % MoS_2 and 1 wt % CNTs were also prepared by the same procedure.

2.3. Characterization. X-ray diffraction (XRD) (Japan Rigaku D/Max-Ra) was performed using a rotating-anode X-ray diffractometer equipped with a Cu Kα tube and a Ni filter (λ = 0.1542 nm) at 40 kV. The data was collected on powder and in reflection orientation. The scanning scope was 5−65° and scanning rate was 4° min^{-1}. Scanning electron microscopy (SEM) (JSM-6800F, JEOL) was used to observe the morphology of the CNTs and MoS_2−CNT hybrids. Transmission electron microscopy (TEM) (Hitachi model H-800) and Energy-dispersive X-ray spectroscopy (EDX) were carried out to observe the morphology and analysis the element composition of the samples. The samples were first dispersed well in ethanol by ultrasonication and then dripped on copper grids. In addition, TEM was also performed to observe the dispersion state of the nanofillers in EP nanocomposites. Thermogravimetric analysis (TGA) was carried out on a Q5000 thermoanalyzer instrument (TA Instruments Inc., New Castle, DE) from room temperature to 800 °C at a heating rate of 20 °C min^{-1} under an N_2 flow of 60 mL min^{-1}. The thermal behavior of the EP composites was further studied by Q2000 differential scanning calorimeter (DSC) (TA Instruments Inc., USA). About 5 mg of samples were heated from 30 to 220 °C at a linear heating rate of 10 °C min^{-1} and kept at 220 °C for 10 min and then cooled at a linear rate of 10 °C min^{-1} from 220 to 30 °C. This heating−cooling cycle was performed once again, and the data was got from the second heating cycle. Dynamic mechanical analysis (DMA) (DMA Q800, TA Instruments Inc.) was carried out in the temperature range from 25 to 250 °C at a heating rate of 5 °C min^{-1} with a frequency of 10 Hz. The combustion properties of EP and EP composites were performed on a microscale combustion calorimeter (MCC-2, GOVMARK).[33] The thermogravimetric analysis/infrared spectrometry (TG-IR) of the samples was carried out using a TGA Q5000 IR thermogravimetric analyzer.[33] Field-emission scanning electron microscopy (FESEM) (JEOL JSM-2010) was performed to observe the micromorphology of the char residues. Raman spectroscopy was performed with a SPEX-1403 laser Raman spectrometer (SPEX Co, U.S.A.).[29] X-ray photoelectron spectroscopy (XPS) was carried out with a VG ESCALB MK-II electron spectrometer (Al Kα excitation source at 1486.6 eV).

3. RESULT AND DISCUSSION

3.1. Characterization of MoS_2−CNTs. Figure 1 shows the XRD patterns of the acid-treated CNTs, synthesized MoS_2 nanolayers, and MoS_2−CNT hybrids. In the XRD pattern of CNTs, the peaks at 25.9° (002) and 42.8° (100) are attributed to the hexagonal graphite structure. For the as-prepared MoS_2, it is very interesting to observe that the (002) diffraction peak at 14.0° disappeared; only three weak and wide diffraction peaks assigned to (100), (103), and (110) planes of MoS_2 were

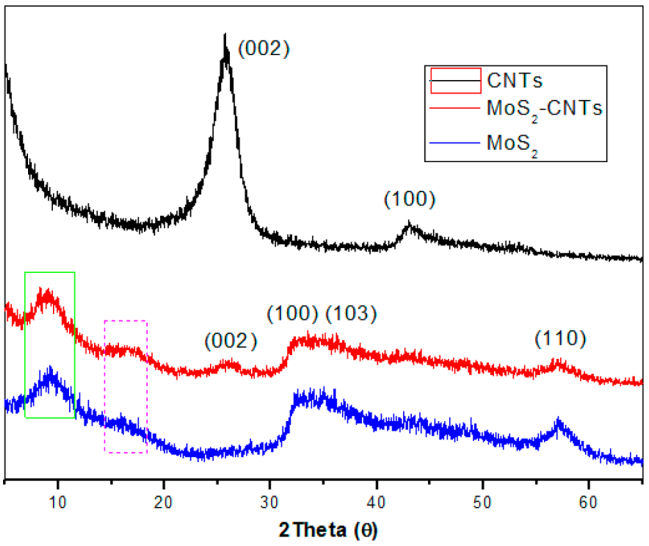

Figure 1. XRD patterns of acid treatment CNTs, MoS_2 nanosheets, and MoS_2−CNT hybrids.

shown.[43,47] The XRD pattern of the MoS_2−CNT hybrids exhibits all diffraction peaks related to the as-prepared MoS_2. In addition, a weak diffraction peak around 25° attributed to the (002) plane of the CNTs was observed. The above results indicated that the MoS_2 nanosheets in the as-prepared MoS_2 and MoS_2−CNT hybrids did not show with restacking structure and they all were composed of a single or few layers of MoS_2.[43] In addition, two new weak diffraction peaks that were instructed by green and purple rectangular wireframe could be observed around 2θ = 9 and 16°. These two diffraction peaks in MoS_2-based hybrids were assigned to the increasing in the distance of the original MoS_2 layers which is good in agreement with previous research work by Chang et al.[44] Moreover, the intensity of the diffraction peaks of CNTs decreased obviously, indicating MoS_2 nanosheets densely covered on the surface of CNTs.[45]

Raman spectrum was further used to investigate the structural of MoS_2−CNT hybrids (Figure S1). The Raman spectrum of CNTs shows the D band at 1350 cm^{-1} that corresponded to scattering from local defects or disorders present in the CNTs, and the G bands at 1585 cm^{-1} which originates from the in-plane tangential stretching of the C−C bonds in the graphitic structure.[48] As for the MoS_2−CNT hybrids, it is notable that besides the typical D band and G band of CNTs, there are two additional characteristic bands of MoS_2, which correspond to the E_{2g} and A_{1g} modes, respectively.[46] The Raman spectrum of the MoS_2−CNT hybrids show the characteristic bands of both CNTs and MoS_2, confirming the presence of CNTs and MoS_2 in the hybrids.

The SEM images of CNTs and MoS_2−CNT hybrids are shown in Figure S2 in the Supporting Information. Figure S2a in the Supporting Information shows a typical SEM image of the CNTs which keep their intact structure after concentrated sulfuric acid and nitric acid treatment. It can be observed from Figure S2b in the Supporting Information that the layered MoS_2 has been successfully grown on a continuous CNTs network. Furthermore, it can also be observed that the morphology of the MoS_2−CNT hybrids is significantly different compared to that of CNTs. No aggregations of the MoS_2 nanosheets off the CNTs scaffold are observed in the

DOI: 10.1021/acsami.5b00762
ACS Appl. Mater. Interfaces 2015, 7, 6070−6081

nanohybrids, indicating that the MoS_2 nanolayers were fixed stubbornly on the surface of CNTs. The morphology and structure of the MoS_2, CNTs, and MoS_2–CNT hybrids were further characterized by TEM (Figure 2). Figure 2a presents a typical TEM image of MoS_2 nanosheets, which is thin layers folded and tangled together. Figure 2b shows the CNTs still keep their original tube structure and the diameter is 20–30 nm. Figure 2c, d further shows the morphology of the MoS_2–CNTs nanohybrids, indicating that the layered MoS_2 with few layers deposits on the surface of CNTs. During the hydrothermal process, CNTs serve as the substrate for the nucleation and growth of MoS_2 into a layered structure because of the interaction between the functional group of CNTs surface and Mo precursors. The elemental compositions of the selected fields (rectangular area in Figure 2d) were determined by EDX, as shown in Figure 2e. It was observed that Cu, C, O, Mo, and S elements existed in Figure 2e. The Cu peaks were originated from the Cu grids. Accordingly, the presence of C and O is contributed from the CNTs and oxygen-containing functional groups of the acid-modified CNTs. The atomic ratio of Mo and S is agreed with the stoichiometry of MoS_2, which can be obtained from the table inserted in Figure 2e. The EDX spectra further confirmed that the MoS_2–CNT hybrids were successfully fabricated.

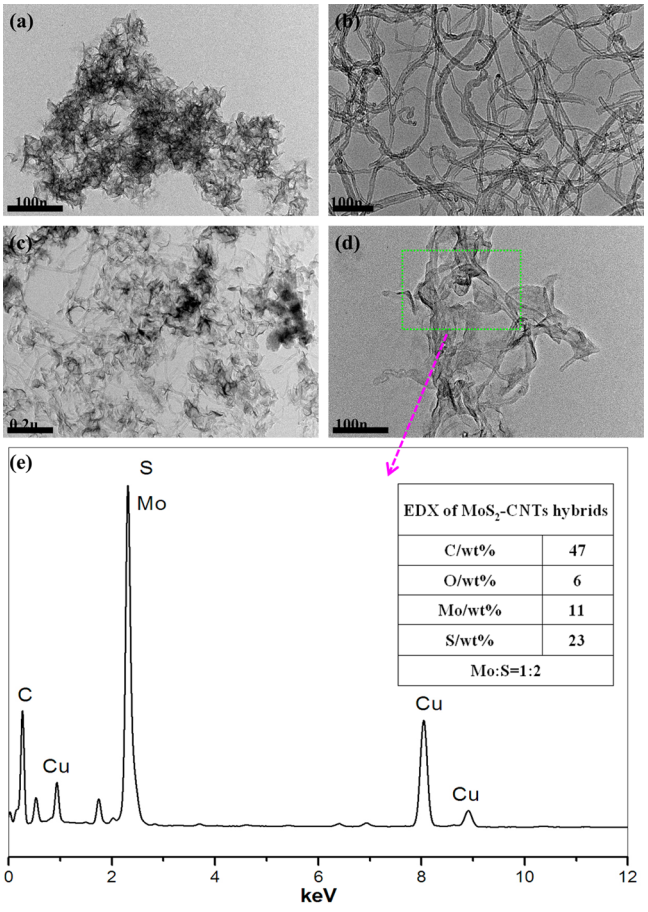

Figure 2. TEM images of (a) MoS_2 nanosheets, (b) acid treatment CNTs and (c, d) MoS_2–CNT hybrids, (e) EDX result of MoS_2–CNT hybrids.

In addition, a dark-field scanning transmission electron microscopy (STEM) was further carried out to observe the structure of MoS_2–CNT hybrids. It could be obviously shown in Figure 3 that the MoS_2 nanolayers were decorated on the surface of CNTs and EDX element mapping of the same structures further showed the spatial distributions of C, Mo, and S in MoS_2–CNT hybrids. The strong C signal across the nanotubes confirmed the existence of CNTs, the Mo and S element detected in the nanolayers visibly suggested the formation of MoS_2.

3.2. Dispersion State of CNTs and MoS_2–CNTs Hybrids in EP Composites. To the best of our knowledge, the dispersion and interface interaction of nanofillers in polymer matrix are two critical factors for optimizing the improvement of the performances of polymer nanocomposites.[49] Therefore, it is of great significance to study the dispersibility of CNTs in the EP nanocomposites. The dispersion states of CNTs and MoS_2–CNT hybrids in EP matrix were observed by means of TEM, as shown in Figure 4. It was observed that the acid-treated CNTs agglomerated

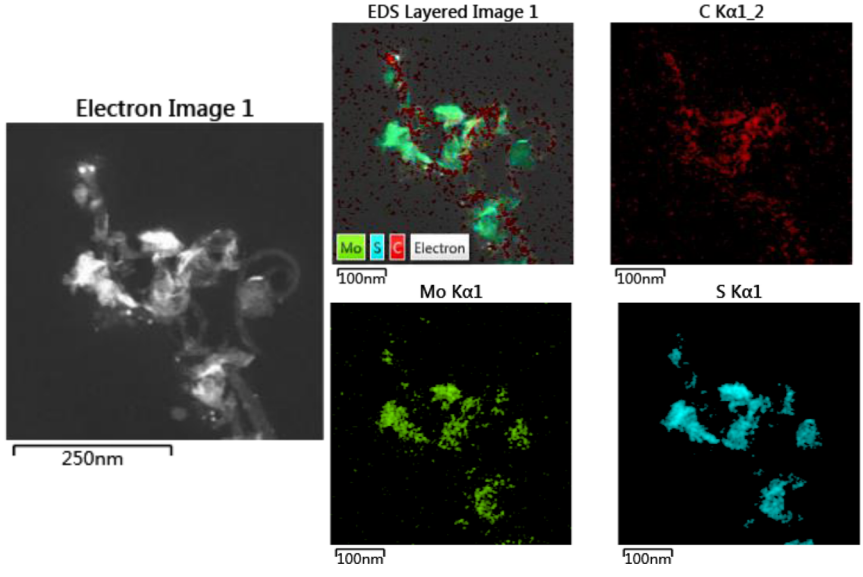

Figure 3. STEM analysis and EDX element mapping of MoS_2–CNT hybrids.

DOI: 10.1021/acsami.5b00762
ACS Appl. Mater. Interfaces 2015, 7, 6070–6081

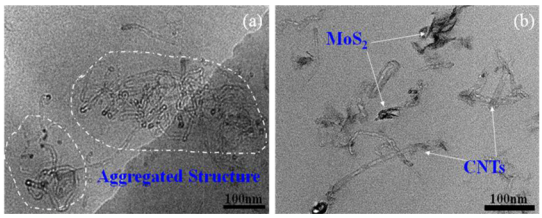

Figure 4. TEM ultrathin observations of the (a) EP/2% CNTs composites and (b) EP/2% MoS_2−CNTscomposites.

seriously in the EP matrix with a curled, entangled, and bundled structure under higher magnification because of the van der Waals force between CNTs (Figure 4a). In contrast, the attachment of MoS_2 nanolayers on the CNTs promotes the dispersion of CNTs in EP matrix effectively and no obvious aggregation of CNTs was observed (Figure 4b), which are mainly due to the MoS_2 nanolayers deposited on the surface of CNTs acting as barriers in preventing the restacking and agglomeration of the CNTs. Obviously, the decorating of MoS_2 nanolayers on CNTs surface was an effective method to improve the dispersion of CNTs in the polymer matrix. In addition, some of the MoS_2 nanolayers are no longer attached to the CNT surface, probably because of ultrasonication, stirring, and shearing during the preparation of nanocomposites.[50]

3.3. Thermal Behavior of EP and Its Composites. The glass transition temperature (T_g) of the nanocomposites is an important parameter that can be used to characterize the effect of the filler on the thermo-viscoelasticity and the physical properties of the polymer matrix.[51] The T_g of EP and its composites were measured by DSC and the results are presented in Table 1. The DSC curves of EP and its composites are presented in Figure S3 in the Supporting Information. Compared to pristine EP, the samples containing CNTs, MoS_2 and MoS_2−CNTs showed a high T_g, which demonstrates that the addition of CNTs, MoS_2 and MoS_2−CNTs can promote the degree of cure.[52] In addition, the increase in T_g is attributed to the fact that the presence of MoS_2 nanolayers and the CNTs network structure restrict the molecular mobility to some degree. For the EP/2% MoS_2−CNTs composites, the increase in T_g is more obvious than EP/2% CNTs composites. It is mainly attributed to the good dispersion of nanofillers in the EP matrix, which can result in a strong confinement effect.[53]

Table 1. DSC, TGA, and MCC Results of EP and EP Composites

sample	T_g (°C)	$T_{-10\%}$ (°C)	T_{max} (°C)	char residue[a] (%)	PHRR (Wg^{1-})	THR (kJ g^{-1})
EP	130	376	386	13.6	337	40.3
EP/2% MoS_2	151	355	366	20.0	318	35.6
EP/2% CNTs	145	366	377	19.7	298	33.2
EP/2% MoS_2−CNTs	158	343	369	22.2	248	27.7
EP/1% MoS_2/1% CNTs	148	343	357	21.6	284	30.1

[a]At 700 °C.

TGA was used to investigate the thermal stability of EP and EP composites. TG-DTG profiles and the corresponding data for EP and its composites under nitrogen atmosphere are shown in Figure 5 and Table 1, respectively. As can be observed, all the nanocomposites present similar degradation behaviors to that of pristine EP. The thermal decomposition process of pure EP and EP composites only contains one stage referred to the DTG profile, which is mainly ascribed to the decomposition of the macromolecular chains. For the EP/MoS_2, EP/CNTs and EP/MoS_2−CNTs composites, their temperature of the initial degradation ($T_{-10\%}$: the temperature of 10 wt % weight loss) and the temperature of maximum weight loss rate (T_{max}) is lower than that of pure EP, which were attributed to the earlier thermal degradation of MoS_2, functional groups on the acid treatment CNTs or the high thermal conductivity of CNTs.[52] However, the addition of MoS_2−CNT hybrids shows higher char residues compared to EP, EP/MoS_2, and EP/CNTs composites, which reaches up to 22.2%. The char residues can provide a protective shield of mass and heat transfer, which slow down the heat release rate during combustion, indicating the MoS_2−CNT hybrids can improve the thermal resistance of the EP composite. Moreover, it can be obtained from DTG profiles that the maximum mass loss rate (the peak of DTG curve) of the EP/MoS_2−CNTs composites is lower than that of neat EP, EP/CNTs, and EP/MoS_2 composites, suggesting that MoS_2−CNT hybrids function as an effective barrier to inhibit the mass loss during the thermal degradation process.[53]

3.4. Heat Release of EP and EP Composites. In previous work, the addition of CNTs and MoS_2 individually could impart the flame retardant properties to polymers.[7−9,27−29,31−33] It is shown that the combination of two or more components can provide an incredible fire resistance to polymers because of the synergistic effect. Therefore, MoS_2−CNT hybrids are expected to enhance the fire resistance of EP composites more obvious than CNTs and MoS_2 solely. To confirm this inference, the MCC based on oxygen consumption calorimetry was used to investigate the flammability of EP and EP composites.[54] The PHRR and THR are the key factors for evaluating fire safety. The HRR and THR curves of the EP and EP composites with MoS_2, CNTs, and MoS_2−CNT hybrids are shown in Figure 6 and the related data are shown in Table 1. It can be observed that the flame retardancy of all nanocomposites had improved and CNTs were more effective in reducing the PHRR than MoS_2, which may be caused by the formation of the network structure of CNTs. Moreover, the MoS_2−CNT hybrids could confer more excellent flame retardancy on EP composites compared with MoS_2 and CNTs. The addition of 2 wt % MoS_2−CNT hybrids leads to a 27 and 31% reduction in PHRR and THR, respectively, compared with those of neat EP. The ability of MoS_2−CNT hybrids to improve the flame retardancy of polymer is mainly attributed to create a protective barrier on the surface of the polymer matrices and the free radical trapping effect of the CNTs network, which slow down the heat and mass transfer between gas and condensed phases, and inhibit the underlying polymer composites from further combustion.[8] In detail, the network structured layers formed by CNTs in the polymer matrix could not only isolate polymers from external radiation and heat feedback from the fire zone, but also could act as effective thermal insulation layers.[55] However, the flame retardant efficiency is closely related to the dispersion of nanofillers in polymer matrix, so the decoration of layered MoS_2 on CNTs can prevent CNTs from aggregating and consequently improve the flame retardant efficiency. In addition, MoS_2 also has a flame retardacy effect due to the

DOI: 10.1021/acsami.5b00762
ACS Appl. Mater. Interfaces 2015, 7, 6070−6081

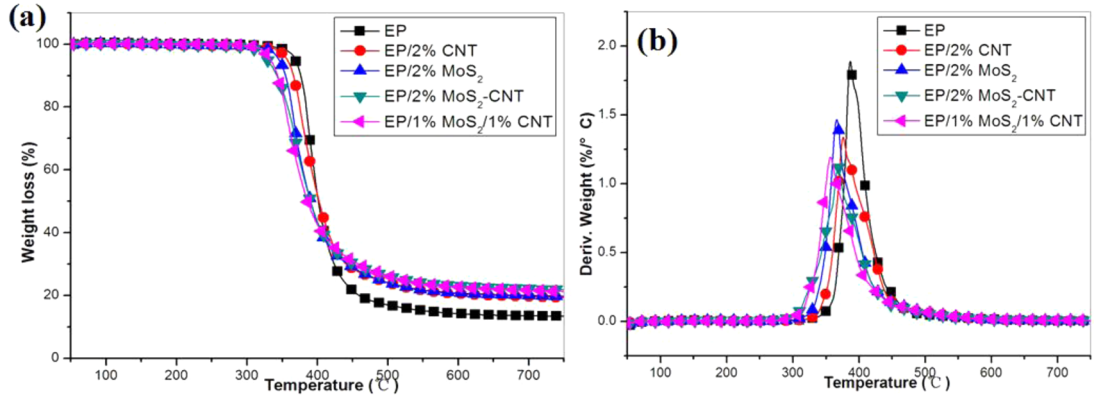

Figure 5. TGA curves of pure EP, EP/2% CNTs, EP/2% MoS_2, EP/2% MoS_2−CNTs, and EP/1% MoS_2/1% CNT composites in nitrogen atmosphere.

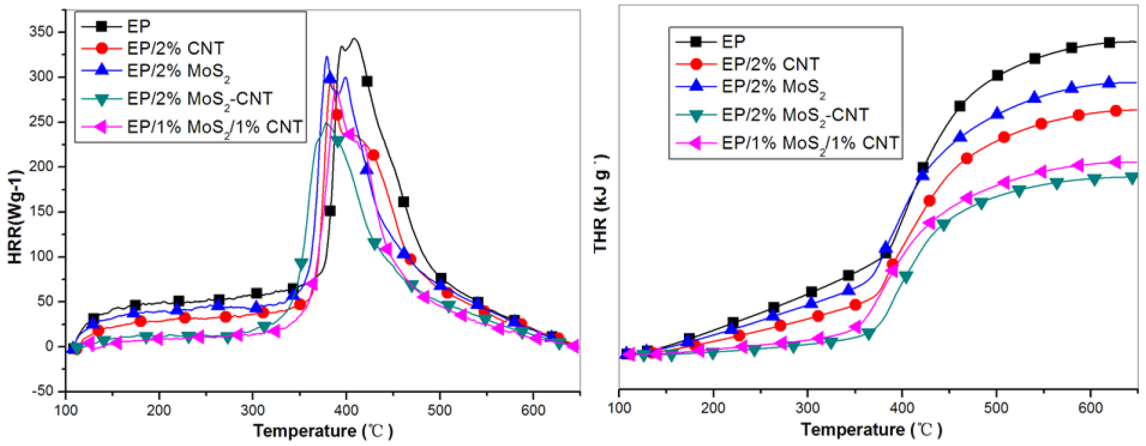

Figure 6. (a) HRR and (b) THR curves of pure EP, EP/2% CNTs, EP/2% MoS_2, EP/2% MoS_2−CNTs, and EP/1% MoS_2/1% CNT composites.

physical barrier effect of the MoS_2 layers and the barrier effect of char residues catalyzed by MoS_2.[29,33]

3.5. Flame Retardant Mechanism. Flame retardants in polymer matrices may act either in condensed phase or in gas phase or also in both phases together. Therefore, TG-FTIR was first selected to analyze the gas volatiles during thermal degradation process. FTIR spectra obtained at the maximum evolution rate during the thermal degradation of EP and EP/MoS_2−CNTs composites are shown in Figure 7a. Some gaseous volatiles evolved from EP and EP/MoS_2−CNTs composites are labeled accurately by characteristic FTIR signals, such as CO_2 (2360 cm^{-1}), CO (2180 cm^{-1}), −C-H groups for allyl alcohol, acetone, ethers and various hydrocarbons (2800−3100 cm^{-1}), aromatic compounds (1605, 1510, and 1460 cm^{-1}).[56] It is observed that the thermal degradation process of the EP/MoS_2−CNTs composites is similar to that of neat EP which is good in agreement with TGA results. However, the intensity of gas emission of EP/MoS_2−CNTs composites is much lower than that of the neat EP. In addition, the differences between EP and EP/MoS_2−CNTs composites are studied by the Gram-Schmidt (GS) curves which are presented in Figure 7b. It is clearly observed that the absorbance intensity of the decomposition products from EP/MoS_2−CNTs is much lower than that from pure EP (for comparison purposes, the absorbance intensity values were normalized by the total mass loss in the TGA).

To further study the changes of the pyrolysis products, the absorbance of gas products for EP and EP/MoS_2−CNTs composites is shown in Figure 7c−f. It can be observed that the absorbance intensity of the pyrolysis products for EP/MoS_2−CNTs is lower than that of EP, including hydrocarbons (Figure 7c), aromatic compounds (Figure 7d), CO_2 (Figure 7e), and CO (Figure 7f). The decrement of hydrocarbons and aromatic compounds leads to a reduction in the HRR, which is in accordance with MCC results. Consequently, the addition of MoS_2−CNT hybrids decreases the volume of combustible gas and weight loss, which is in agreement with thermal analysis results. The reduction of organic gaseous products further gives rise to inhibit the formation of the smoke, because the volatiles are easily cracked into smaller hydrocarbons and smoke particles. The gaseous hydrocarbons are very easy to condense and the smoke particles aggregate to form smoke.[54] Additionally, CO_2 (Figure 7e) and CO (Figure 7f) production for EP/MoS_2−CNTs is much lower than that of neat EP, which is mainly attributed to the improvement of char formation, the physical barrier effect of the MoS_2 nanolayers, and CNT network structure.

Meanwhile, according to previous research works, many kinds of nanofillers, including CNTs, clay, or polyhedral silsesquioxanes, can act as "char reinforcers" or "char expanders" in the condensed phase. When the flame retardants play a role in condensed phase, the flame retardant efficiency mainly depends on the composition and structure of the char. Thus, studying the morphologies and the structure of the obtained char layers will provide insight into understanding how flame retardants play a role in the condensed phase.[56]

DOI: 10.1021/acsami.5b00762
ACS Appl. Mater. Interfaces 2015, 7, 6070−6081

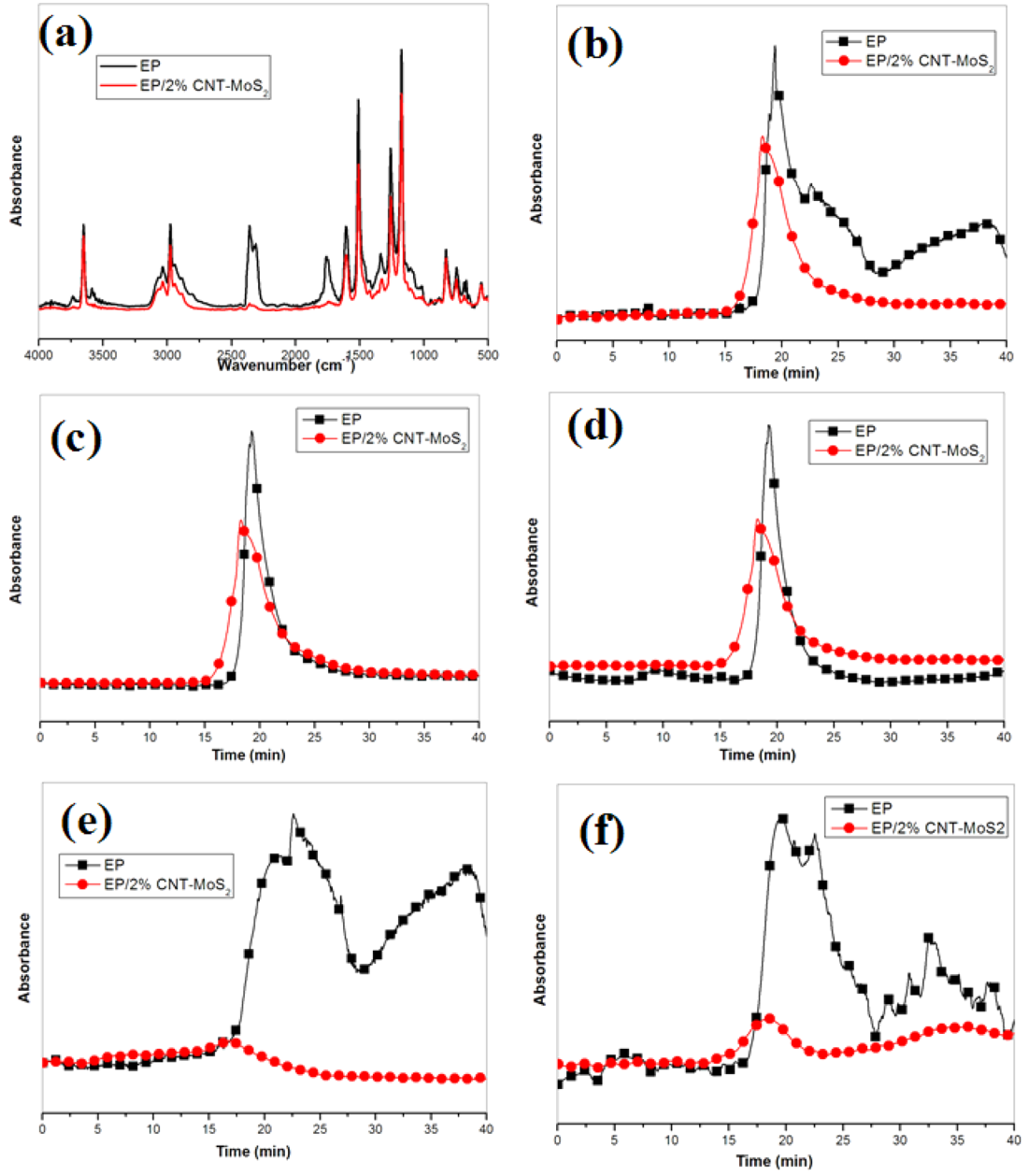

Figure 7. TG-IR results of EP and EP/2% MoS_2−CNTs composites: (a) FT-IR spectrum of pyrolysis products at the maximum decomposition rate, (b) Gram−Schmidt curves, (c) hydrocarbons, (d) aromatic compounds, (e) CO_2, and (f) CO.

The microstructure of the char residues were investigated by SEM to get more information about the char residues after thermal degradation and the corresponding SEM images are shown in Figure 8. As can be observed in Figure 8a, neat EP shows a discontinuous char layer with a large amount of cracks and holes. However, after addition of 2% MoS_2, CNTs and the MoS_2−CNT hybrids into EP, the number of cracks and holes decreased obviously (Figure 8b−d) and the porous and incompact surface changed into more dense, especially for the EP composites with MoS_2−CNT hybrids. It means that the addition of MoS_2−CNT hybrids results in the formation of compact carbonaceous char, which provided a more effective protecting layer during combustion. The compact char layer can effectively inhibit the transferring of heat and volatiles due to the strong barrier effect, and thus provide a good barrier for the underlying material, leading to the impressive enhancement of the thermal stability and fire resistance of the EP nanocomposites.

The microstructure of chars is a key factor for improving the fire resistance of polymers. For a flame retardant system with CNTs, the degree of graphitization reflects the transition extent of carbon material from a turbostratic to graphitic structure.[25] Raman spectroscopy is then used to prove the existence of carbonaceous char in the residue and further analyze the special component of the char. Figure S4 in the Supporting Information shows the Raman spectra of the residual char of EP, EP/2% MoS_2, EP/2% CNTs, and EP/2% MoS_2−CNTs, which are obtained by calcinating the samples in muffle furnace at 600 °C for 15 min and tested directly without acid treatment. It can be observed that all of the spectra exhibit a G and D band at about 1595 and 1365 cm^{-1}, respectively, indicating the char structures. The former is corresponding to the stretching

DOI: 10.1021/acsami.5b00762
ACS Appl. Mater. Interfaces 2015, 7, 6070−6081

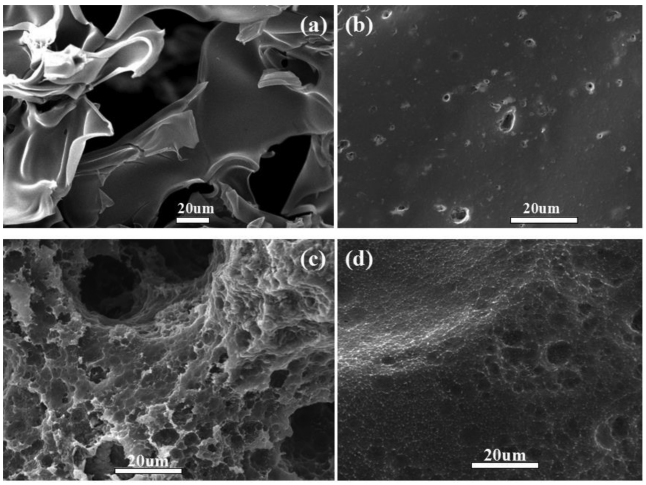

Figure 8. SEM images of the final char residues of EP and EP composites: (a) pure EP; (b) EP/2% MoS_2; (c) EP/2% CNTs; (d) EP/2% MoS_2−CNTs.

vibration mode with E_{2g} symmetry in the aromatic layers of the graphite crystalline, whereas the latter represents disordered graphite or glassy carbons.[29]

The graphitization degree of the char can be calculated by a ratio of the D band intensity and G band intensity (I_D/I_G), where I_D and I_G represents the integrated intensities of the D and G bands, respectively. Basically, the lower the ratio of I_D/I_G, the better structure of the char is. As shown in Figure S4 in the Supporting Information, the I_D/I_G ratio follows the sequence of EP/2% MoS_2−CNTs (2.62) < EP/2% CNTs (2.67) < EP/2% MoS_2 (2.73) < EP (2.84), which indicates the EP/2% MoS_2−CNTs composites have a higher graphitization degree and the most thermally stable char structure. The lower degree of graphitization in the char has relatively high reactivity to oxidation, leading to the char burnt out in the long time exposure to a high extent of heat flux.[25] It can be inferred that the high content of graphitized carbons in the residual char is known to be compact and efficient in terms of thermal insulation, which can provide an effective shield that results in a decrease in heat and mass transfers between the flame and the material. The result of Raman spectroscopy confirms the graphitization degree of the EP/2% MoS_2−CNTs composites is higher than that of the EP and the EP composites with MoS_2 or CNTs solely, resulting in the enhancement of the thermal properties and flame retardance of the composites, which is in accordance with the SEM results.

The exterior and interior residual char of EP and EP/2% MoS_2−CNTs composites are further investigated by XPS analysis, and the corresponding results are presented in Figure 9. The characteristic C_{1s} bands at 284.6, 286.8, and 288.4 eV are attributed to C−H and C−C in aliphatic and aromatic species, C−O (ether and/or hydroxyl group) and C═O, respectively.[56] Moreover, the aliphatic and aromatic species (C−H or C−C) concentration no matter in the exterior or interior residual char of EP/2% MoS_2−CNTs composites is higher than that in the exterior and interior char residues of pure EP, respectively, implying that the char residues of EP/2% MoS_2−CNTs composites with a higher graphitization degree. To further study the thermal oxidative resistance of the char residues, we calculated C_{ox}/C_a (C_{ox}, oxidized carbons and C_a, aliphatic and aromatic carbons) values.[57] The C_{ox}/C_a values of the exterior and interior residual char of EP/2% MoS_2−CNTs composites are 0.32 and 0.22, respectively, which are much lower than those of EP. Furthermore, the Mo and a small amount of S element can be detected, implying that the MoS_2 nanolayers have been oxidized to molybdenum oxide, which can efficiently suppress the production of smoke.[58]

In a word, it is very interesting to observe the combination of CNTs and MoS_2 nanolayers shows a synergistic effect in improving the fire resistance of EP. The mechanism of the improved flame retardancy for EP/MoS_2−CNTs composite is illustrated in Scheme 1. There are three possible reasons for the enhancement of fire resistance of EP by incorporating MoS_2−CNT hybrids, that is, (1) physical effect of CNTs and MoS_2 nanolayers, (2) chemical effect of MoS_2, and (3) the combination of physical effect and chemical effect. It is well-known that the incorporation of CNTs into polymer matrices is easy to form a three-dimensional networklike structure resulting in a higher melt viscosity that can lead to excellent flame retardancy.[8] Most importantly, incorporating MoS_2 nanolayers functionalized CNTs results in a further improvement in fire resistance of EP composites rather than CNTs. This can be ascribed to the diameter of MoS_2 nanolayers functionalized CNTs is larger than that of pure CNTs, and thus the coexistence of MoS_2 and CNTs in the composites form a more effective confined space and enhances the network structure; on the other hand, nanocomposites with good dispersion exhibit much higher complex viscosity than those with poor CNTs dispersion because poorly dispersed CNTs lead to formation of a discontinuous layer that consists of fragmented islands rather than the continuous network protective layer.[59] In detail, the network structured layers formed by CNTs could not only shield polymers from external radiation and heat feedback from the fire zone, but also could effectively impedes transport of oxygen and flammable volatiles, and greatly inhibits the combustion process of the materials. In addition, the flame retardancy of the EP composites is also closely dependent on the physical barrier effect and catalytic carbonization effect of MoS_2 nanolayers. The dense and continuous char layer and MoS_2 nanolayers are good barriers to protect the underlying materials; reduce the diffusion of volatile combustible fragments; and inhibit the exchange of combustible gases, degradation products, and oxygen.

3.6. Mechanical Properties Performed by DMA. The above research results have demonstrated the synergistic effect in improving the thermal stability and flame retardancy of EP through the combination of MoS_2 nanolayers and CNTs. Moreover, it is attractive as a nonhalogen method for improving fire resistance of polymer composites without sacrificing mechanical properties simultaneously. The influence of CNTs and MoS_2−CNT hybrids on the mechanical properties of the EP composite is evaluated using DMA. Storage modulus curves (a) and loss angle tangent (b) of the pure EP and its composites are shown in Figure S5 in the Supporting Information. After incorporating CNTs into the EP matrix, the storage modulus of all the EP composites increases. However, MoS_2−CNT hybrids show much higher increase in storage modulus compared with CNTs. The same tendency is found in T_g values, which are defined as the temperature at maximum of tan δ. The T_g values of EP, EP/2% MoS_2, EP/2% CNTs, and EP/2% MoS_2−CNTs are 155, 167, 164, and 172 °C, respectively, which are in accordance with the DSC results.[60] The increase in T_g indicates that the movement of polymer chains is confined. In this work, the increase in T_g values can be mainly ascribed to the nanotube network, which

DOI: 10.1021/acsami.5b00762
ACS Appl. Mater. Interfaces 2015, 7, 6070−6081

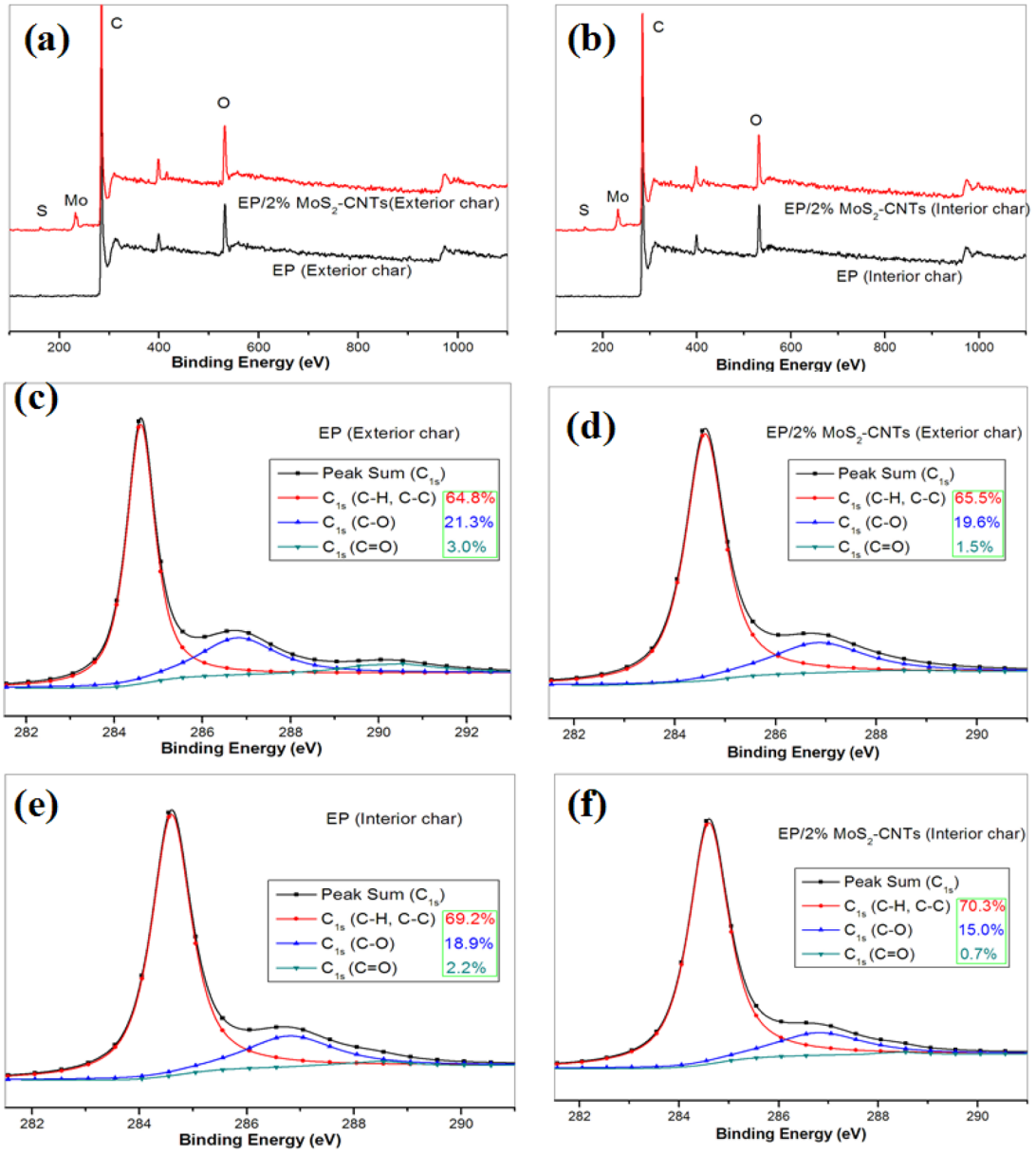

Figure 9. XPS survey of the char residues of EP and EP/2% MoS_2−CNTs composites.

limits the movement of molecule chains. It is well-known that the well dispersion CNTs is conducive to form a compact network structure. The more compact the nanotube network, the more difficult the movement of polymer chains, and consequently, the higher the T_g value. Moreover, the MoS_2 nanolayers can restrict the segmental motion of the polymer chains in the nanocomposites which result in higher T_g in EP/2% MoS_2 composites. As discussed with the morphology of the sample EP/2% MoS_2−CNTs (Figure 4), the existence of good dispersed states of CNTs and MoS_2 nanolayers in the EP matrix obviously reinforces the EP matrix and reflects into the modulus values and T_g.

4. CONCLUSION

In summary, this work herein reported a facile strategy to prepare MoS_2 nanolayer-wrapped CNT hybrids, and its composition and structure were characterized by XRD, Raman spectra, SEM, and TEM. The morphological study exhibited that MoS_2 nanolayers were decorated on the surface of CNTs. The MoS_2−CNT hybrids were well-dispersed in the EP matrix, leading to remarkable improvement of thermal stability, flame retardancy, and mechanical properties. Incorporation of 2 wt % MoS_2−CNT hybrids into EP resulted in the increase in char yield and decrease in DTG peak value compared to neat epoxy. Moreover, the combination of CNTs and MoS_2 nanolayers can further reduce the PHRR, THR, and inhibit the combustion process of EP compared with the addition of CNTs or MoS_2 alone in EP matrix. In addition, the amount of organic volatiles was obviously reduced, and the toxic carbon monoxide was suppressed after incorporating MoS_2−CNT hybrids, which demonstrated MoS_2 and CNTs had a synergistic effect on reducing fire hazards. A possible flame retardant mechanism was illustrated based on the analyses of pyrolysis products and char residues. In gas phase, the presence of MoS_2−CNT hybrids acts as a physical barrier that could slow down and decrease the release volume of combustible gas, especially hydrocarbons and aromatic compounds; in the condensed phase, the addition of MoS_2−

DOI: 10.1021/acsami.5b00762
ACS Appl. Mater. Interfaces 2015, 7, 6070−6081

Scheme 1. Proposed Flame Retardant Mechanism of MoS_2–CNT Hybrids in Epoxy Composites

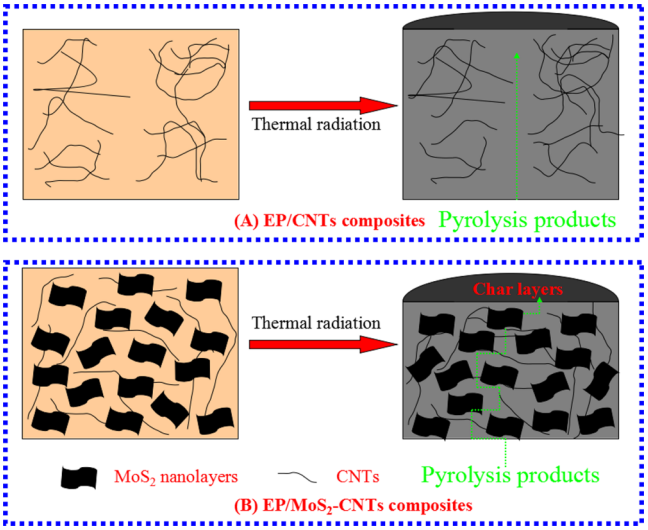

CNT hybrids led to forming a compact and insulating char layer to protect the inner polymer matrix from further burning. The approach demonstrated herein is a promising strategy for simultaneously improving the fire resistance and mechanical properties of polymer composites.

■ ASSOCIATED CONTENT

Ⓢ Supporting Information

Additional figures (Raman spectrum, SEM images, DSC curves and DMA curves). This material is available free of charge via the Internet at http://pubs.acs.org/.

■ AUTHOR INFORMATION

Corresponding Authors

*E-mail: yuanhu@ustc.edu.cn. Tel.: +86-551-63601664. Fax: +86-551-3601664.

*E-mail: zgui@ustc.edu.cn. Tel.: +86-551-63601288. Fax: +86-551-3601669.

Notes

The authors declare no competing financial interest.

■ ACKNOWLEDGMENTS

This work was supported by the National Basic Research Program of China (973 Program) (2012CB719701), National Basic Research Program of China (973 Program) (No.2012CB922002) and National Key Technology R&D Program (2013BAJ01B05).

■ REFERENCES

(1) Chen, L.; Chai, S. G.; Liu, K.; Ning, N. Y.; Gao, J.; Liu, Q. F.; Chen, F.; Fu, Q. Enhanced Epoxy/Silica Composites Mechanical Properties by Introducing Graphene Oxide to the Interface. *ACS Appl. Mater. Interfaces* **2012**, *4*, 4398−4404.

(2) Zhang, X.; He, Q. L.; Gu, H. B.; Colorado, H. A.; Wei, S. Y.; Guo, Z. H. Flame-Retardant Electrical Conductive Nanopolymers Based on Bisphenol F Epoxy Resin Reinforced with Nano Polyanilines. *ACS Appl. Mater. Interfaces* **2013**, *5*, 898−910.

(3) Wang, X.; Xing, W. Y.; Feng, X. M.; Yu, B.; Song, L.; Hu, Y. Functionalization of Graphene with Grafted Polyphosphamide for Flame Retardant Epoxy Composites: Synthesis, Flammability and Mechanism. *Polym. Chem.* **2014**, *5*, 1145−1154.

(4) Gérard, C.; Fontaine, G.; Bellayer, S.; Bourbigot, S. Reaction to Fire of an Intumescent Epoxy Resin: Protection Mechanisms and Synergy. *Polym. Degrad. Stab.* **2012**, *97*, 1366−1386.

(5) Liu, S.; Yan, H. Q.; Fang, Z. P.; Wang, H. Effect of Graphene Nanosheets on Morphology, Thermal Stability and Flame Retardancy of Epoxy Resin. *Compos. Sci. Technol.* **2014**, *90*, 40−47.

(6) Liu, S.; Yan, H. Q.; Fang, Z. P.; Guo, Z. H.; Wang, H. Effect of Graphene Nanosheets and Layered Double Hydroxides on the Flame Retardancy and Thermal Degradation of Epoxy Resin. *RSC Adv.* **2014**, *4*, 18652−18659.

(7) Ma, H. Y.; Tong, L. F.; Xu, Z. B.; Fang, Z. P. Functionalizing Carbon Nanotubes by Grafting on Intumescent Flame Retardant: Nanocomposite Synthesis, Morphology, Rheology, and Flammability. *Adv. Funct. Mater.* **2008**, *18*, 414−421.

(8) Kashiwagi, T.; Du, F. M.; Douglas, J. F.; Winey, K. I.; Harris, R. H.; Shields, J. R. Nanoparticle Networks Reduce the Flammability of Polymer Nanocomposites. *Nat. Mater.* **2005**, *4*, 928−933.

(9) Peeterbroeck, S.; Laoutid, F.; Taulemesse, J. M.; Monteverde, T.; Lopez-Cuesta, J. M.; Nagy, J. B.; Alexandre, M.; Dubois, P. Mechanical Properties and Flame-Retardant Behavior of Ethylene Vinyl Acetate/High-Density Polyethylene Coated Carbon Nanotube Nanocomposites. *Adv. Funct. Mater.* **2007**, *17*, 2787−2791.

(10) Cipiriano, B. H.; Kashiwagi, T.; Raghavan, S. R.; Yang, Y.; Grulke, E. A.; Yamamoto, K.; Shields, J. R.; Douglas, J. F. Effects of Aspect Ratio of MWNT on the Flammability Properties of Polymer Nanocomposites. *Polymer* **2007**, *48*, 6086−6096.

(11) Schartel, B.; Potschke, P.; Knoll, U.; Abdel-Goad, M. Fire Behaviour of Polyamide 6/Multiwall Carbon Nanotube Nanocomposites. *Eur. Polym. J.* **2005**, *41*, 1061−1070.

(12) Bocchini, S.; Frache, A.; Camino, G.; Claes, M. Polyethylene Thermal Oxidative Stabilisation in Carbon Nanotubes Based Nanocomposites. *Eur. Polym. J.* **2007**, *43*, 3222−3235.

(13) Kashiwagi, T.; Grulke, E.; Hilding, J.; Groth, K.; Harris, R.; Butler, K.; Shields, J.; Kharchenko, S.; Douglas, J. Thermal and Flammability Properties of Polypropylene/Carbon Nanotube Nanocomposites. *Polymer* **2004**, *45*, 4227−4239.

(14) Biagio, D. V.; Patrizia, L.; Giovanni, S.; Vincenzo, T.; Liberata, G.; Marialuigia, R.; Luigi, V.; Vittoria, V. Improvement of the Electrical Conductivity in Multiphase Epoxy-Based MWCNT Nanocomposites by means of an Optimized Clay Content. *Compos. Sci. Technol.* **2013**, *89*, 69−76.

(15) Liu, L.; Grunlan, J. C. Clay Assisted Dispersion of Carbon Nanotubes in Conductive Epoxy Nanocomposites. *Adv. Funct. Mater.* **2007**, *17*, 2343−2348.

(16) Zhu, J.; Peng, H.; Rodriguez-Macias, F.; Margrave, J. L.; Khabashesku, V. N.; Imam, A. M.; Lozano, K.; Barrera, E. Reinforcing Epoxy Polymer Composites Through Covalent Integration of Functionalized Nanotubes. *Adv. Funct. Mater.* **2004**, *14*, 643−648.

(17) Caroline, G.; Gaëlle, F.; Serge, B. Synergistic and Antagonistic Effects in Flame Retardancy of an Intumescent Epoxy Resin. *Polym. Adv. Technol.* **2011**, *22*, 1085−1090.

(18) Chattopadhyay, D. K.; Webster, D. C. Thermal Stability and Flame Retardancy of Polyurethanes. *Prog. Polym. Sci.* **2009**, *34*, 1068−1133.

(19) He, Q. L.; Yuan, T. T.; Yan, X. R.; Ding, D. W.; Wang, Q.; Luo, Z. P.; Shen, T. D.; Wei, S. Y.; Cao, D. P.; Guo, Z. H. Flame-Retardant Polypropylene/Multiwall Carbon Nanotube Nanocomposites: Effects of Surface Functionalization and Surfactant Molecular Weight. *Macromol. Chem. Phys.* **2014**, *215*, 327−340.

(20) Coleman, J. N. Liquid-Phase Exfoliation of Nanotubes and Graphene. *Adv. Funct. Mater.* **2009**, *19*, 3680−3695.

(21) Han, Z.; Zhang, F.; Lin, D.; Xing, B. Clay Minerals Affect the Stability of Surfactant-Facilitated Carbon Nanotube Suspensions. *Environ. Sci. Technol.* **2008**, *42*, 6869−6875.

(22) Pack, S.; Kashiwagi, T.; Stemp, D.; Koo, J.; Si, M.; Sokolov, J. C.; et al. Segregation of Carbon Nanotubes/Organoclays Rendering Polymer Blends Self-Extinguishing. *Macromolecules* **2009**, *42*, 6698−6709.

DOI: 10.1021/acsami.5b00762
ACS Appl. Mater. Interfaces 2015, 7, 6070−6081

(23) Wang, Z.; Meng, X.; Li, J.; Du, X.; Li, S.; Jiang, Z.; et al. A Simple Method for Preparing Carbon Nanotubes/Clay Hybrids in Water. *J. Phys. Chem. C* **2009**, *113*, 8058−8064.
(24) Palza, H.; Reznik, B.; Wilhelm, M.; Arias, O.; Vargas, A. Electrical, Thermal, and Mechanical Characterization of Poly(propylene)/Carbon Nanotube/Clay Hybrid Composite Materials. *Macromol. Mater. Eng.* **2012**, *297*, 474−480.
(25) Ma, H.; Tong, L.; Xu, Z.; Fang, Z. Synergistic Effect of Carbon Nanotube and Clay for Improving the Flame Retardancy of ABS Resin. *Nanotechnology* **2007**, *18*, 1−8.
(26) Song, P. A.; Zhao, L. P.; Cao, Z. H.; Fang, Z. P. Polypropylene Nanocomposites Based on C_{60}-decorated Carbon Nanotubes: Thermal Properties, Flammability, and Mechanical properties. *J. Mater. Chem.* **2011**, *21*, 7782−7788.
(27) Zvonimir, M.; Ruchi, S.; Manias, E.; Charles, G. H.; Wilkie, C. A. Polystyrene/Molybdenum Disulfide and Poly(methyl methacrylate)/Molybdenum Disulfide Nanocomposites with Enhanced Thermal Stability. *Polym. Degrad. Stab.* **2012**, *97*, 2481−2486.
(28) Zhou, K. Q.; Yang, W.; Tang, G.; Wang, B. B.; Jiang, S. H.; Hu, Y.; Gui, Z. Comparative Study on the Thermal Stability, Flame Retardancy and Smoke Suppression Properties of Polystyrene Composites Containing Molybdenum Disulfide and Graphene. *RSC Adv.* **2013**, *3*, 25030−25040.
(29) Zhou, K. Q.; Jiang, S. H.; Bao, C. L.; Song, L.; Wang, B. B.; Tang, G.; Hu, Y.; Gui, Z. Preparation of Poly(vinyl alcohol) Nanocomposites with Molybdenum Disulfide (MoS_2): Structural Characteristics and Markedly Enhanced Properties. *RSC Adv.* **2012**, *2*, 11695−11703.
(30) Zhou, K. Q.; Liu, J. J.; Wang, B.; Zhang, Q. J.; Shi, Y. Q.; Jiang, S. H.; Hu, Y.; Gui, Z. Facile Preparation of Poly(methyl methacrylate)/MoS_2 Nanocomposites via In Situ Emulsion Polymerization. *Mater. Lett.* **2014**, *126*, 159−161.
(31) Zhou, K. Q.; Zhang, Q. J.; Liu, J. J.; Wang, B.; Jiang, S. H.; Shi, Y. Q.; Hu, Y.; Gui, Z. Synergetic Effect of Ferrocene and MoS_2 in Polystyrene Composites with Enhanced Thermal Stability, Flame Retardant and Smoke Suppression Properties. *RSC Adv.* **2014**, *4*, 13205−13214.
(32) Zhou, K. Q.; Liu, J. J.; Wen, P. Y.; Hu, Y.; Gui, Z. A Noncovalent Functionalization Approach to Improve the Dispersibility and Properties of Polymer/MoS_2 Composites. *Appl. Surf. Sci.* **2014**, *316*, 237−244.
(33) Zhou, K. Q.; Jiang, S. H.; Shi, Y. Q.; Liu, J. J.; Wang, B.; Hu, Y.; Gui, Z. Multigram-scale Fabrication of Organic Modified MoS_2 Nanosheets Dispersed in Polystyrene with Improved Thermal Stability, Fire Resistance, and Smoke Suppression Properties. *RSC Adv.* **2014**, *4*, 40170−40180.
(34) Zhou, K. Q.; Liu, J. J.; Zeng, W. R.; Hu, Y.; Gui, Z. In Situ Synthesis, Morphology, and Fundamental Properties of Polymer/MoS_2 Nanocomposites. *Compos. Sci. Technol.* **2015**, *107*, 120−128.
(35) Zhang, X.; Alloul, O.; He, Q. L.; Zhu, J. H.; Verde, M. J.; Li, Y. T.; Wei, S. Y.; Guo, Z. H. Strengthened Magnetic Epoxy Nanocomposites with Protruding Nanoparticles on the Graphene Nanosheets. *Polymer* **2013**, *54*, 3594−3604.
(36) Tchoul, M. N.; Ford, W. T.; Lolli, G.; Resasco, D. E.; Arepall, S. Effect of Mild Nitric Acid Oxidation on Dispersability, Size, and Structure of Single-Walled Carbon Nanotubes. *Chem. Mater.* **2007**, *19*, 5765−5772.
(37) Gao, C.; Muthukrishnan, S.; Li, W.; Yuan, J.; Xu, Y.; Muller, H. E. Linear and Hyperbranched Glycopolymer-Functionalized Carbon Nanotubes: Synthesis, Kinetics, and Characterization. *Macromolecules* **2007**, *40*, 1803−1815.
(38) Stanley, S. C.; Mrinmoy, De.; Jaemyung, K.; Segi, B.; Conner, D.; Yu, J.; Huang, J. X.; Vinayak, P. D. Ligand Conjugation of Chemically Exfoliated MoS_2. *J. Am. Chem. Soc.* **2013**, *135*, 4584−4587.
(39) Zhou, L.; He, B. Z.; Yang, Y.; He, Y. G. Facile Approach to Surface Functionalized MoS_2 Nanosheets. *RSC Adv.* **2014**, *4*, 32570−32578.
(40) Song, P.; Liu, L.; Fu, S.; Yu, Y.; Jin, C.; Wu, Q.; Zhang, Y.; Li, Q. Striking Multiple Synergies Created by Combining Reduced Graphene Oxides and Carbon Nanotubes for Polymer Nanocomposites. *Nanotechnology* **2013**, *24*, 1−8.
(41) Li, Y.; Yang, T.; Yu, T.; Zheng, L.; Liao, K. Synergistic Effect of Hybrid Carbon Nanotube-Graphene Oxide as a Nanofiller in Enhancing the Mechanical Properties of PVA Composites. *J. Mater. Chem.* **2011**, *21*, 10844−10851.
(42) Song, P. A.; Liu, L. N.; Huang, G. B.; Yu, Y. M.; Guo, Q. P. Largely Enhanced Thermal and Mechanical Properties of Polymer Nanocomposites via Incorporating C_{60}@Graphene Nanocarbon Hybrid. *Nanotechnology* **2013**, *24*, 1−8.
(43) Park, S. K.; Yu, S. H.; Woo, S.; Quan, B.; Lee, D. C.; Kim, M. K.; Sung, Y. E.; Y Piao, Y. Z. A Simple L-cysteine-Assisted Method for the Growth of MoS_2 Nanosheets on Carbon Nanotubes for High-Performance Lithium Ion Batteries. *Dalton Trans.* **2013**, *42*, 2399−2405.
(44) Chang, K.; Chen, W.; Ma, L.; Li, H.; Li, H.; Huang, F.; Xu, Z.; Zhang, Q.; Lee, J. Y. Graphene-like MoS_2/Amorphous Carbon Composites with High Capacity and Excellent Stability as Anode Materials for Lithium Ion Batteries. *J. Mater. Chem.* **2011**, *21*, 6251−6257.
(45) Huang, K. J.; Wang, L.; Zhang, J. Z.; Wang, L. L.; Mo, Y. P. One-step preparation of Layered Molybdenum Disulfide/Multi-walled Carbon Nanotube Composites for Enhanced Performance Supercapacitor. *Energy* **2014**, *67*, 234−240.
(46) Kartick, B.; Suneel, K. S.; Sourindra, M. MoS_2-MWCNT Hybrids as a Superior Anode in Lithium-Ion Batteries. *Chem. Commun.* **2013**, *49*, 1823−1825.
(47) Huang, G. C.; Chen, T.; Chen, W. X.; Wang, Z.; Chang, K.; Ma, L.; Huang, F. H.; Chen, D. Y.; Lee, J. Y. Graphene-Like MoS_2/Graphene Composites: Cationic Surfactant-Assisted Hydrothermal Synthesis and Electrochemical Reversible Storage of Lithium. *Small* **2013**, *9*, 3693−3703.
(48) Yang, M. Q.; Weng, B.; Xu, Y. J. Synthesis of In_2S_3-CNT Nanocomposites for Selective Reduction under Visible Light. *J. Mater. Chem. A* **2014**, *2*, 1710−1720.
(49) Bao, C. L.; Guo, Y. Q.; Song, L.; Kan, Y. C.; Qian, X. D.; Hu, Y. In Situ Preparation of Functionalized Graphene Oxide/Epoxy Nanocomposites with Effective Reinforcements. *J. Mater. Chem.* **2011**, *21*, 13290−13298.
(50) Zhou, K. Q.; Wang, B.; Liu, J. J.; Jiang, S. H.; Shi, Y. Q.; Zhang, Q. J.; Hu, Y.; Gui, Z. The Influence of α-FeOOH/rGO Hybrids on the Improved Thermal Stability and Smoke Suppression Properties in Polystyrene. *Mater. Res. Bull.* **2014**, *53*, 272−279.
(51) Ketan, S.; Khare, F. K.; Rajesh, K. Effect of Carbon Nanotube Functionalization on Mechanical and Thermal Properties of Cross-Linked Epoxy-Carbon Nanotube Nanocomposites: Role of Strengthening the Interfacial Interactions. *ACS Appl. Mater. Interfaces* **2014**, *6*, 6098−6110.
(52) Yu, H. O.; Liu, J.; Wen, X.; Jiang, Z. W.; Wang, Y. J.; Wang, L.; Zheng, J.; Fu, S. Y.; Tang, T. Charing Polymer Wrapped Carbon Nanotubes for Simultaneously Improving the Flame Retardancy and Mechanical Properties of Epoxy Resin. *Polymer* **2011**, *52*, 4891−4898.
(53) Feng, X. M.; Xing, W. Y.; Song, L.; Hu, Y. In Situ Synthesis of a MoS_2/CoOOH Hybrid by a Facile Wet Chemical Method and the Catalytic Oxidation of CO in Epoxy Resin during Decomposition. *J. Mater. Chem. A* **2014**, *2*, 13299−13308.
(54) Dong, Y. Y.; Gui, Z.; Hu, Y.; Wu, Y.; Jiang, S. H. The Influence of Titanate Nanotube on the Improved Thermal Properties and the Smoke Suppression in Poly(methyl methacrylate). *J. Hazard. Mater.* **2012**, *209*, 34−39.
(55) Du, B. X.; Fang, Z. P. The Preparation of Layered Double Hydroxide Wrapped Carbon Nanotubes and their Application as a Flame Retardant for Polypropylene. *Nanotechnology* **2010**, *21*, 315603.
(56) Wang, X.; Zhou, S.; Xing, W. Y.; Yu, B.; Feng, X. M.; Song, L.; Hu, Y. Self-assembly of Ni-Fe Layered Double Hydroxide/Graphene Hybrids for Reducing Fire Hazard in Epoxy Composites. *J. Mater. Chem. A* **2013**, *1*, 4383−4390.
(57) Bourbigot, S.; LeBras, M.; Delobel, R.; Gengembre, L. XPS Study of an Intumescent Coating II. Application to the Ammonium

DOI: 10.1021/acsami.5b00762
ACS Appl. Mater. Interfaces 2015, 7, 6070−6081

Polyphosphate/ Pentaerythritol/Ethylenic Terpolymer Fire Retardant System with and without Synergistic agent. *Appl. Surf. Sci.* **1997**, *120*, 15−29.
(58) Li, B. A Study of the Thermal Decomposition and Smoke Suppression of Poly(vinyl chloride) Treated with Metal Oxides Using a Cone Calorimeter at a High Incident Heat Flux. *Polym. Degrad. Stab.* **2002**, *78*, 349−356.
(59) Kashiwagi, T.; Du, F. M.; Winey, K. I.; Groth, K. M.; Shields, J. R.; Bellayer, S. P.; Douglas, J. F. Flammability Properties of Polymer Nanocomposites with Single-Walled Carbon Nanotubes: Effects of Nanotube Dispersion and Concentration. *Polymer* **2005**, *46*, 471−481.
(60) Jiang, S. H.; Gui, Z.; Hu, Y.; Zhou, K. Q.; Dong, Y. Y.; Shi, Y. Q. The Intercalation of Poly(methyl methacrylate)/Aluminophosphate Nanocomposites and the Properties Improvement. *Mater. Chem. Phys.* **2013**, *141*, 95−100.

DOI: 10.1021/acsami.5b00762
ACS Appl. Mater. Interfaces 2015, 7, 6070−6081